Published in final edited form as:
Somatosens Mot Res. 2009 December ; 26(4): 90–104. doi:10.3109/08990220903335742.

Functional connectivity for somatosensory and motor cortex in spastic diplegia

Harold Burton[1,2], **Sachin Dixit**[2], **Patricia Litkowski**[1], and **Jason R. Wingert**[3]

[1]Department of Anatomy and Neurobiology, Washington University School of Medicine, St Louis, MO, USA

[2]Department of Radiology, Washington University School of Medicine, St Louis, MO, USA

[3]Department of Health and Wellness, University of North Carolina at Asheville, Asheville, NC, USA

Abstract

Functional connectivity (fcMRI) was analyzed in individuals with spastic diplegia and age-matched controls. Pearson correlations (*r*-values) were computed between resting state spontaneous activity in selected seed regions (sROI) and each voxel throughout the brain. Seed ROI were centered on foci activated by tactile stimulation of the second fingertip in somatosensory and parietal dorsal attention regions. The group with diplegia showed significantly expanded networks for the somatomotor but not dorsal attention areas. These expanded networks overran nearly all topological representations in somatosensory and motor areas despite a sROI in a fingertip focus. A possible underlying cause for altered fcMRI in the group with dipegia, and generally sensorimotor deficits in spastic diplegia, is that prenatal third trimester white-matter injury leads to localized damage to subplate neurons. We hypothesize that intracortical connections become dominant in spastic diplegia through successful competition with diminished or absent thalamocortical inputs. Similar to the effects of subplate ablations on ocular dominance columns (Kanold and Shatz, Neuron 2006;51:627–638), a spike timing-dependent plasticity model is proposed to explain a shift towards intracortical inputs.

Keywords

Magnetic resonance imaging; diplegia; humans; spontaneous activity

Introduction

Cerebral palsy (CP) is a neurodevelopmental disorder occurring in approximately 1.5–2.5 per 1000 live births (Kuban and Leviton 1994; Sigurdardóttir et al. 2009). The prevalence rises particularly with premature births during the third trimester—between 24 and 32 gestational weeks (Himmelmann et al. 2005). CP involves axonal and neuronal losses in cerebral white and gray matter, reduction in thalamocortical connections (Hoon et al. 2002, 2009; Thomas et al. 2005; Nagae et al. 2007), and comparable losses in subcortical structures (Volpe 2009). Spastic diplegia, a common CP subtype, is most often characterized by non-progressive periventricular white-matter injury (PWMI) (Kulak et al. 2007; Leviton and Gressens 2007; Korzeniewski et al. 2008) involving diffuse poorly visualized lesions or frank cystic white-matter damage (Kuban and Leviton 1994; Volpe 2009).

Correspondence: Dr H. Burton, Department of Anatomy and Neurobiology, Campus Box 8108, Washington University School of Medicine, 660 South Euclid Avenue, St Louis, MO 63110, USA. Tel: +1 314 362 3556. Fax: +1 314 747 4370. harold@pcg.wustl.edu.

In addition to subcortical abnormalities, PWMI injures developing cortical synaptic circuitry (Kuban and Leviton 1994; Back et al. 2001, 2005) and cerebral cortical organization (Volpe 2009). The lesions alter neuronal migration between the ventricular (germinal) zone and developing cortical plate, and reduce neurogenesis, gliogenesis, and differentiation within the subventricular zone, the main source of subplate and interneurons in human cerebral cortex (Zecevic et al. 2005). Damage to subplate neurons disrupts crucial trophic influences on GABAergic neurons, their migration to the cortical plate, maturation of inhibitory synapses in cortical layer 4, and refinement of thalamocortical synapse formation (Ghosh and Shatz 1993; Kanold et al. 2003; McQuillen and Ferriero 2005; Kanold and Shatz 2006; Robinson et al. 2006; Leviton and Gressens 2007; Kostovic and Jovanov-Milosevic 2008; Volpe 2009). An example of possible impaired functioning of cortical interneurons, and thereby reduced cortical inhibitory function in children with spastic diplegia, was suggested by findings of shortened postexcitatory potentials following stimulation of the corticospinal tract (Vry et al. 2008). However, there is limited information on the consequences of these neurodevelopmental disorders on cortical activity in spastic diplegia.

Indicative of abnormal brain organization in spastic diplegia is motor deficits, especially in the lower extremities (Palisano et al. 2000; Rosenbaum et al. 2002), and disturbed sensory, perceptual, communication, and cognitive functions (Gorter et al. 2004; Bax et al. 2005; Sanger and Kukke 2007; Wingert et al. 2008, 2009a; Hoon et al. 2009). Mildly affected spastic diplegia patients can ambulate independently and are typically cognitively and intellectually normal. However, all four limbs show significantly diminished tactile, joint-position sense, and kinesthesia compared to age-matched controls even in minimally impacted individuals (Wingert et al. 2008, 2009a). In a functional magnetic resonance imaging (fMRI) study with controlled tactile stimulation in mildly affected spastic diplegia individuals, we found smaller response magnitudes and constricted spatial extents especially in primary and secondary somatosensory cortex (Wingert et al. 2009b).

On the basis of these psychophysical data, imaging findings, and clinically identified motor deficits, we hypothesized that the cortical networks linked to areas within the somatosensory and motor cortices would be disordered in spastic diplegia compared to normal controls. The direction of change, however, was not predictable. The diminished tactile-evoked activity found in the fMRI study might suggest smaller networks. Thus, a factor in the sensory deficits might be reduced size of cortical networks involved in sensory discriminative processing.

Another alternative is that intracortical connections might come to dominate in spastic diplegia through successful competition with reduced thalamocortical inputs. This notion derives from a neuroplasticity model developed in studies of ocular dominance columns in visual cortex of kittens following *in utero* destruction of subplate neurons (Kanold and Shatz 2006). Maturation of inhibitory synapses failed in subplate-ablated cortex, which postnatally resulted in a paradoxical shift towards visual cortex activation from weaker visually deprived eye inputs. The PWMI damage to the subplate zone might have comparable effects in spastic diplegia and lead to greater influence from intracortical connections. Thus, clinical symptoms of motor deficits might suggest some breakdown in the topography within and between somatosensory and motor areas, which might be expected to indicate unregulated network expansions within and between these regions. Thus, disruptions in the internal somatotopy within somatosensory regions might indicate less ability to focus on inputs to selected parts of the body; and the feed forward of sensory information to motor cortex might be expressed as motor deficits in spastic diplegia.

A measure of cortical networks is provided by functional connectivity analyses (fcMRI). Cortical networks determined with functional connectivity reliably predict the distribution of cortical areas activated in conventional task-related imaging studies (Vincent et al. 2006,

2007) even in the presence of cerebral lesions (Quigley et al. 2001). Examples of cortical networks studied using fcMRI in humans are the somatomotor (Biswal et al. 1995; Cordes et al. 2000; De Luca et al. 2005; Fox et al. 2006b), attention (Fox et al. 2006a), "defaultmode" (Greicius et al. 2003; Fox et al. 2005), language (Cordes et al. 2000; Hampson et al. 2002), memory (Hampson et al. 2006; Vincent et al. 2006), and command/task control systems (Dosenbach et al. 2007). Somatosensory and motor networks were analyzed in the current study using foci in those cortical areas identified in prior studies that specifically included individuals with spastic diplegia (Wingert et al. 2009b). Prior fcMRI studies have successfully determined cortical organization disruptions in patient populations showing spatial neglect following strokes and where the extent and duration of disruption correlated with the severity of spatial neglect (He et al. 2007). These studies suggest that functional connectivity network differences can be explored in spastic diplegia where symptomology includes somatosensory and motor deficits.

Methods

Participants

Twenty-three individuals provided informed consent following guidelines approved by the Human Studies Committee of Washington University. Twelve had spastic diplegia (5 females; mean age = 20 years, SEM = 1.8); gestational age at birth was between 24 and 31 weeks (mean = 27.8 weeks, SEM = 2.5). Eleven age-matched individuals were without neurological or orthopedic disabilities (4 females; mean age = 20 years, SEM = 1.9). Those with spastic diplegia were mildly affected and had homogeneous clinical presentations with relatively similar encephalopathy. Motor weakness and spasticity affected both legs more than the arms, as is typical of spastic diplegia. All ambulated without assistance, which classified them as level I or II on the Gross Motor Function Classification (Palisano et al. 2000); they also were scored level I or II in the Manual Ability Classification System (Eliasson et al. 2006). They were of normal intelligence and were not medicated for spasticity.

All but two of the current group with spastic diplegia participated in prior somatosensory psychophysical (Wingert et al. 2008, 2009a) and functional magnetic imaging studies (Burton et al. 2007; Wingert et al. 2009b). The ten spastic diplegia participants studied previously were significantly less accurate when performing tactile objection–recognition tasks and had higher thresholds when judging roughness differences between tactile gratings (Wingert et al. 2008).

Image acquisition

Images based on blood-oxygenation-level-dependent (BOLD) contrast responses (Kwong et al. 1992; Ogawa et al. 1992) were acquired in a Siemens 3 Tesla TRIO scanner (Erlangen, Germany). BOLD response images were based on gradient recalled echo-planar sequences (EPI: repetition time [TR] = 2200 ms, echo time [TE] = 27 ms, flip angle = 90°). Axially aligned EPI image slices paralleled the bicommissural plane; whole brain coverage was obtained across 36 contiguous, interleaved 4mm slices with in-plan resolution of 4mm × 4mm. Additionally, two structural images were acquired. One was T2-weighted and obtained across 36 slices that were in-register with the EPI (TR = 8430 ms, TE = 98 ms, resolution was 1.33mm × 1.33mm × 3mm). The second was a higher resolution T1-weighted magnetization prepared rapid gradient echo (MP-RAGE) scan acquired across 176 sagittal slices (TR = 2100 ms, TE = 3.93 ms, flip angle = 7°, inversion time [TI] =1000 ms, resolution was 1mm × 1mm × 1.25 mm).

Images were obtained using a standard RF head coil with the head stabilized by a vacuum cushion. The eyes were covered by a blindfold, which did not fully obscure room lights. Participants were instructed to keep their eyes open during the structural scans. The room lights were off during EPI scans and participants were instructed to remain awake with their eyes

closed; no task was performed. Spontaneous brain activity was recorded in successive EPI runs. One hundred and sixty-four image volumes were collected for each run. Room lights were turned on for ~ 1 min between each run. During breaks between runs, participants were instructed to open their eyes and queried regarding whether they remained awake during the preceding run.

Image processing

Images from each participant were passed through previously described processing (Fox et al. 2005, 2006a; Vincent et al. 2006, 2008). Initial steps corrected for systematic time shifts between slices, eliminated intensity differences due to interleaved odd–even slice acquisition, normalized whole brain mean signal intensity to mode 1000 across EPI runs, and corrected alignment due to inter-frame head motion within and across runs. EPI images from each run were then registered to an atlas template by computing 12 parameter affine transforms that linked the average of the first EPI volumes across runs with the T2- and T1-weighted structural images (Ojemann et al. 1997). The atlas representative structural template was based on an average of MP-RAGE images from 48 normal young individuals (22.5 ± 3 years) (Buckner et al. 2004) and made to conform to Talairach atlas space (Talairach and Tournoux 1988) using prior spatial normalization methods (Lancaster et al. 1995). The atlas template was deemed appropriate for the spastic diplegia group because none of the spastic diplegia participants showed substantial structural distortions on their MP-RAGE images. Eleven individuals had a diffuse type of PWMI; one case had small bilateral cystic lesions. All cases had slight to modest bilateral enlargement of the lateral ventricles.

To prepare the BOLD/EPI data, images were transformed to atlas space and resampled to 2mm cubic voxels. The images were spatially smoothed (6mm full width at half-maximum) and temporally band-pass filtered to remove frequencies >0.1 Hz. The data was also modified through linear regression to remove nine sources of nuisance variance and their associated temporal derivatives. These included six linear corrections for head movement, a global whole brain signal averaged over all voxels in atlas space, and non-neuronal signals in the ventricles and white matter. The latter two signals were averages individually extracted in each participant from ventricle and white-matter regions across successive structural image slices that were selected using Analyze (Mayo Research Foundation, Rochester, MN, USA). The ventricle region extended from the fourth to lateral ventricles; the white-matter region was bilateral and located superior to the lateral ventricles.

Correlation computations

Correlation analyses were done in the volumetrically normalized images for each individual. The correlations were between the time series in seed ROI and the time series in all other brain voxels. The time series were based on concatenation across runs excluding time points at run starts for magnetization stabilization. Seed ROI (sROI) were 12mm diameter spheres centered on selected coordinates (Table I).[1] The time series from each sROI was the average across all voxels within the sphere.

The coordinates for each sROI were determined from surface-based registration of somatosensory-evoked activity in a prior study involving spastic diplegia and control participants (Wingert et al. 2009b). The coordinates were the centers of mass on surface-based conjunction maps (CMs). The CMs included cortical areas that were multiple-comparison corrected, thresholded sites[2] of significant activation during three different discrimination tasks

[1]The coordinates for sROI were averages across spastic diplegia and control groups based on the results of a prior functional imaging study of tactile activated sites (Wingert et al. 2009b). The averages were based on ten control participants unique to the prior fMRI study and data from nine current spastic diplegia participants who also were in the prior study.

that involved tactile stimulation of the right index finger. CMs reflected the constellation of nodes where ≥60% of the participants in either group showed significant activity during any task (Friston et al. 1999). An exclusive intersection of CMs and nodes included in previously defined cortical areas specified ROIs. Coordinates listed in Table I are the centers of mass for the surface areas representing the inclusion of CMs in defined cortical areas. Previously defined cortical areas included portions of Brodmann areas 3, 1, and 2 that were confined to the finger representation (Maldjian et al. 1999), the OP 1 subdivision of the parietal operculum (Burton et al. 2008b), and regions overlying intraparietal sulcal cortex (BA7) previously associated with tactile attention (Burton et al. 2008a). All defined cortical areas were deformed to the standard PALS-B12 atlas.

The individual regression coefficient maps were computed (Vincent et al. 2006) and converted to a normal distribution by Fischer's **Z**-transform (Jenkins and Watts 1968). These **Z**-transforms were then divided by the square root of the variance[3] to create a voxel-wise Gaussian *Z*-distribution (with zero mean and unit variance).

Surface-based registration of data

Structural and functional data from every participant were registered to a standard, population-average, surface-based atlas (Van Essen 2005) that provided a common space for group comparisons. The registration process first involved creating participant-specific surfaces for each hemisphere using a segmentation boundary midway through cortical gray matter with the Surefit method (Van Essen et al. 2001). These participant-specific surface reconstructions approximated the course of cortical layer four in that individual (Van Essen 2005). The volumetric corrected *z*-values were then registered to participant-specific surface nodes. Next, participant surfaces were deformed to the distribution of nodes in the PALS-B12 atlas; the deformation relied on aligning the spherical coordinates for six highly consistent anatomical landmarks individually identified in a participant hemisphere to the same land-marks in the average PALS-B12 atlas sphere (Van Essen 2005). The landmarks were the central sulcus, calcarine sulcus, superior circular sulcus within the Sylvian fissure, anterior half of the superior temporal gyrus, and dorsal and ventral segments of the medial wall.[4] The deformation matrices obtained from landmark-based registration that were created for each participant were deployed to register *z*-values from the nodes of each participant-specific surface to the PALS-B12 atlas nodes. The registration to the "standard mesh" facilitated alignment of data to corresponding locations from different individuals (Nordahl et al. 2007). We then computed the average per node of aligned *z*-scores associated with a particular sROI for each group. To assess the group level statistical probability of these node-wise maps, conventional random effects *t*-score maps were computed (Holmes and Friston 1998).

Group contrast analyses—surface registered data

Cluster size analysis—A *t*-statistic was computed to determine group differences in the corrected *z*-score values per participant that were registered to the PALS-B12 atlas surface. The purpose was to determine whether the connectivity network for a selected sROI differed significantly between groups. These *t*-statistic maps were visualized using *p*-value thresholds of 0.05–0.0005 (one-tailed *t*-values 1.7–3.8 for 21 df). The analysis was conducted separately

[2]The threshold criteria in a GLM analysis of volumetric data for corrected z-scores was $p = 0.05$ for $z = 3.0$, 3.5, 4.0, and 4.5 over, respectively, at least 45, 24, 12, and 5 face-connected voxels. The voxels passing threshold were binary coded and subsequently registered to the PALS-B12 atlas mesh (Burton et al. 2008a).

[3]Variance was computed as $1/\sqrt{(\text{degrees of freedom} - 3)}$. The degrees of freedom (df) were corrected because individual time points from a BOLD time series lack independence. The correction according to Bartlett's theory (Jenkins and Watts 1968) involves a Gamma factor (GF) computed from auto-correlation functions (ACRs). GF is the average of the integrals of the ACRs for each of several seed ROIs for every participant. The computed GFs for 7 diplegia and 7 normal participants and 15 sROI did not significantly differ (two-tailed *t*-test, $p = 0.28$). The corrected df was calculated as [(number of BOLD runs * number of functional frames)/GF)].

[4]http://brainvis.wustl.edu/help/landmarks_core6/landmarks_core6.html

for each hemisphere and included data from 12 spastic diplegia and 11 control participants. Significance in each of these *t*-maps was evaluated using a permutation cluster size analysis (Nichols and Holmes 2002)[5] whose purpose was to identify the area(s) of significant clusters (see below) based on the distribution of permuted *t*-maps. For each of 5000 permutations, the 23 fcMRI *z*-score maps were randomly shuffled before computing a new *t*-map. The resulting 5000 *t*-maps were thresholded at ±2.83 ($p = 0.01$ for 21 df). A significant cluster represented contiguous nodes with suprathreshold *t*-values. The surface areas of all clusters were computed and the area of the smallest of the 250 largest clusters in the permuted *t*-maps (5000 iterations × alpha = 0.05) was used as the cluster size threshold for significance. The cluster area in the original *t*-map that exceeded the cluster size threshold was identified and the probability of its size was determined from the permuted distribution. The boundary of a significant cluster was overlaid on the original *t*-statistic map of group contrasts. A separate cluster size analysis was done for fcMRI maps in each hemisphere based on each sROI.

Area extent—An area index metric was used to determine possible group differences in the spatial extents in the connectivity maps for several somato-sensory sROI within selected cortical regions registered to the PALS-B12 surface (Van Essen 2005). Area-proportion indices (API) were based on the ratio of two surface-based areas and were computed for each participant. These surface areas were associated with the fiducial surface for each participant in PALS-B12 space. Consequently, nodes included within a surface area manifested that individual's unique cortical anatomy for the selected nodes (Burton et al. 2008b). The denominator in the ratio was the surface area included within a selected cortical region. The numerator was the area within the selected cortical region that included all nodes whose Bartlett corrected *z*-value threshold was ≥ 3 ($p < 0.003$) for a particular sROI. A random effect Tukey *t*-test evaluated group differences in APIs within each selected cortical region. The *t*-test *p*-values were Bonferroni corrected for testing six regions for each sROI (0.05/6 = 0.008).

Results

Functional connectivity maps

Figure 1 shows functional networks linked to two parietal somatosensory areas: the left BA1 subdivision of S1 and left OP 1 subdivision of S2. In controls, the network for the L BA1 sROI occupied bilaterally the middle of the pre-postcentral gyri, a sliver of the parietal operculum and a patch of left frontal premotor cortex. In diplegia, the L BA1 network encompassed nearly all of the post- and precentral gyri, part of the superior temporal plane, insula, inferior supramarginal cortex, and medial frontal-cingulate cortex.[6] Similar differences in network extent were noted with a sROI in the left OP 1. In controls, the network for L OP 1 included bilaterally all of the parietal operculum, adjoining temporal operculum and insula, inferior supramarginal gyrus, and patches along the left postcentral gyrus. In diplegia, the network extended bilaterally throughout the post- and precentral gyri, parietal and temporal opercula, insula, and a portion of medial frontal and adjoining cingulate cortex (Figure 1). The timecourses in these two sROI completely overlapped in both groups (Figure 2), indicating that the observed network expansions in diplegia were not due to group differences in the magnitudes of resting state MR signals. Seeds placed in BA3 bilaterally and right BA1 showed similar functional connectivity expansions in diplegia (not shown).

The group contrast *t*-test results indicated where the functional connectivity maps in diplegia were larger based on a minimal positive *t*-value threshold of $p = 0.05$. Example *t*-test maps for L BA1 and L OP 1 are shown in Figure 3. For these and all tested sROI, the scarcity of clusters

[5]This surface-based cluster size method is comparable to the suprathreshold cluster test (Nichols and Holmes 2002) and controls against false positive clusters.

[6]Arrows show the position of medial frontal-cingulate cortex on the flattened maps in Figure 1.

with negative *t*-values indicated that there were no loci where controls showed larger network extents.

The permutation analysis of cluster size provided statistical confirmation that the networks in diplegia cases were larger. In Figure 3, clusters whose areas were significantly larger in diplegia are indicated within black borders. For the L BA1 sROI, the boundaries enclosed a significant size cluster that spanned across the pre- and postcentral gyri and much of the parietal operculum (Figure 3). The left pre- and postcentral cortex cluster was 3376mm^2 (Table II, $p = 0.01$) and extended medial and lateral to the finger/hand representation. Additionally for the L BA1 sROI, a second significant cluster was located over the parietal operculum and nearby auditory cortex (Table II, cluster size = 1769.8mm^2, $p = 0.02$). The cluster on the right was less extensive over the pre- and postcentral gyri but also extended as a continuous region over the parietal operculum (Figure 3). The size of the combined cluster was significant (Table II, L BA1, RH, cluster size = 3440mm^2, $p = 0.01$).

Several significant size clusters were found for the L OP 1 sROI (Figure 3). On the left, one of these clusters occupied the pre- and postcentral gyri (Table II, cluster size = 2592.1mm^2, $p = 0.01$); a smaller one was over medial frontal cortex (Table II, cluster size = 1347.2mm^2, $p = 0.03$). On the right, five significant clusters were found (Figure 3) and involved pre- and postcentral gyri, insula, parietal operculcum plus nearby cortex, and medial paracentral plus superior parietal lobule (Table II). The network expansions in diplegia noted for sROI in L and R BA3 and R BA1 mostly resembled those found for L BA1 and L OP 1 and thus involved parietal somatosensory and precentral motor cortex (Table II).

Other parietal cortex sROI showed no or smaller and more localized network expansions in diplegia. For L and R BA2 significant clusters were principally located in medial and superior parietal cortex (Table II). Similarly, significant clusters were more isolated for a sROI in left medial postcentral gyral cortex within Brodmann area 5. For this L BA5 sROI there were no significant clusters in the left hemisphere, indicating comparable networks in both groups. However, diplegia showed more expansive connections in the right hemisphere that included medial postcentral and superior parietal lobule cortex (Table II). There was no evidence of group differences in the networks linked to the left BA7A sROI (Figure 3, Table II). However, the remaining sROI located within the IPS (R BA7A, L BA7P, and R BA7P) showed significant clusters within and superior to the intraparietal cortex (Table II). Cluster sizes for all of these sROI were smaller than those noted for the somatosensory sROI (Table II, 695–958mm^2).

These permutation findings were especially conservative in avoiding false positives in that the boundaries of the significant cluster surrounded only those portions of the random effect *t*-maps with a probability <0.0005 (Figure 3). The *p*-values for several regions within the *t*-test map also were <0.0005; these were not identified as significant in the permutation analysis because their size did not pass the threshold for cluster size.

Area extent measurements

The functional connectivity expansions in diplegia for sROI L BA1 and L OP 1 involved a high proportion of the cortical surface areas defined for several cortical regions. Thus, multiple-comparison corrected results indicated significantly larger APIs in diplegia for ten and nine regions in, respectively, the left and right hemispheres (Table III). For example, the network linked to L BA1 sROI in diplegia occupied a significantly greater proportion of PO, PCG, and BA42 (Heschl's gyrus) bilaterally (Figure 4, Table III). Similarly, the network found for the L BA3 sROI was significantly more extensive in PO and BA42 in diplegia (Table III). The API for PCG approached significance for the L BA3 sROI (Table III, $p = 0.009$). Only the network for the L BA2 sROI had no significant group differences after Bonferroni corrections (Table III). The network tied to L OP 1 sROI occupied significantly greater proportions

bilaterally of the sensory PCG and BA42 areas, frontal cortex BA4 and BA24 motor areas, and left premotor BA6 (Figure 4, Table III). There were no Bonferroni corrected group differences for networks functionally connected to the sROI located in the anterior part of the intraparietal sulcus (L BA7A) (Table III). These API findings indicated that functional connectivity for sROI in S1 and S2 in diplegia involved ~80% of the total areas assigned to left hemisphere sensory regions: S1 (PCG), S2 (PO), and primary auditory (BA42), 40–60% of motor areas (BA4 and BA6), and ~50% of the midline BA24 (Figure 4). In contrast, the APIs in controls for the same sROI were less than 50% of the total area in these same regions (Figure 4).

Discussion

Individuals with spastic diplegia had expanded functional connectivity as compared to controls in somatosensory parts of parietal cortex. Thus, a sROI in any anatomical part of the postcentral gyrus (primary somatosensory area, S1) or the OP 1 subdivision of the parietal operculum (S2) (Eickhoff et al. 2007; Burton et al. 2008b) was functionally connected across >80% of the post-central gyrus and parietal operculum. For example, a sROI isolated to the second fingertip representation in S1 or S2 in the group with diplegia was functionally connected across nearly all body representations in S1 and S2 bilaterally. The networks associated with parietal cortex somatosensory regions also included extensive linkage to precentral motor cortex. Additionally, the functional connectivity maps associated with these same S1 and S2 sROI showed no evidence of topological segregation in frontal cortex motor areas. In contrast, functional connectivity in controls for these same sROI was always more restricted in S1 and motor cortex. One consequence of the more extensive functional connectivity distributions in spastic diplegia was potential disruption to the somatotopic organizations in S1 and S2. Thus, the functional connectivity map associated with a single finger zone in diplegia overlapped nearly all of the somatosensory cortex and thereby likely could influence all topographical somatosensory cortex components.

A second consequence of the expanded functional connectivity in diplegia was lack of any distinctions between the connections associated with sROI in different somatosensory cortex subdivisions. Prior studies have demonstrated that each postcentral gyrus subdivision serves selected somatosensory functions (e.g., Randolph and Semmes 1974) and different intracortical connections (Jones and Powell 1969, 1970; Pearson and Powell 1985; Shanks et al. 1985; Burton and Fabri 1995). The parietal operculum somatosensory subdivisions similarly exhibit different functional characteristics and cortical connections (e.g., Burton et al. 1995, 2008b). Because the networks associated with different somatosensory subdivisions were largely indistinguishable, it is possible that in diplegia the unique processing of somatosensory information provided by different subdivisions is disrupted.

The selected sROI probably represented comparable somatosensory cortical representations for the fingers in both groups, because the seeds were centered on cortical areas where ≥60% of control and spastic diplegia individuals showed evoked responses during three different tactile discrimination tasks with stimulation of the right index finger (Wingert et al. 2009b). Similar parietal cortex coordinates have been identified using tactile stimulation of the right index finger (Maldjian et al. 1999; Burton et al. 2006, 2008a, 2008b). It is possible functional connectivity from other body representations in parietal cortex would not differ in diplegia, especially if these parietal cortex regions were less affected by PWMI.

PWMI observable in the structural images from many of the studied diplegia cases was located within the area of thalamocortical projections to parietal cortex and the functional connectivity expansions in this group principally involved the nearby somatosensory areas. In the present study, there were fewer instances of significantly larger networks in diplegia that were linked to sROI located posterior or medial to the largest extent of the lateral ventricle enlargements.

For example, there were fewer significant clusters in the functional connectivity group contrasts for parietal sROI that were located along the intraparietal sulcal and in medial postcentral gyral cortex within, respectively, Brodmann areas 7 and 5. For these sROI, significant clusters were smaller and primarily confined to posterior/superior parietal cortex. Thus, despite some expansions of functional networks in diplegia, there was less evidence that the networks for these sROI overran multiple subdivisions of S1, S2, or frontal cortex motor areas. These differences in the functional connectivity expansions amongst seed regions might indicate the location and size of PWMI in the studied group.

PWMI leads to subplate damage (McQuillen et al. 2003; McQuillen and Ferriero 2005), which in the current diplegia participants, probably occurred within parietal cortex. The developmental consequences of subplate damage possibly explains the paradoxical finding that in diplegia tactilely evoked activity in somatosensory cortex stimulation was weaker (Wingert et al. 2009b) whereas, as shown here, functional connectivity networks for S1 and S2 were larger. Thus, normally dominating thalamocortical inputs are deficient in diplegia. A similar paradoxical finding was previously described in the visual system when subplate neurons were destroyed *in utero* in kittens, and subsequent deprived eye inputs dominated visual cortex activity (Kanold et al. 2003; Kanold and Shatz 2006). The shift towards deprived eye inputs was explained by alterations in spike timing-dependent plasticity (STDP) that depended on the balance between subplate neuronal and thalamocortical inputs (Kanold and Shatz 2006; Ohshiro and Weliky 2006). The status of somatosensory cortex in diplegia might similarly be shifted towards intracortical inputs due to the combined effects of diminished GABAergic neurons and reduced thalamocortical connections. Severe loss of GABAergic neurons has been observed in autopsies of cerebral palsy brains (Robinson et al. 2006) and GABAergic neuron deficiencies are probable in surviving spastic diplegia cases. Thus, in diplegia parietal sensory neurons do not experience STDP from coincident, reinforcing coherent activation from subplate and thalamocortical neuronal activity. A reduced population of GABAergic interneurons in diplegia also would fail to depress intracortical inputs (Ben-Ari 2002; Kanold and Shatz 2006; Huang et al. 2007). Thus, the neuroplastic influence of long-term depression (LTD) is diminished (Kanold and Shatz 2006; Ohshiro and Weliky 2006). Consequently, synaptic inputs from persisting intracortical linkages are not blocked. Furthermore, relatively normal intracortical connections persist while thalamocortical connections decline (Hoon et al. 2002, 2009; Thomas et al. 2005; Nagae et al. 2007). Possibly expanded intracortical connections (Marin-Padilla 1997) might also be available to compete successfully against diminished thalamocortical inputs, as previously noted in the visual system (Ghosh and Shatz 1993; Kanold et al. 2003). The STDP model then explains how intracortical inputs paradoxically evoke expanded functional connectivity across multiple body representations whereas thalamocortical inputs lead to less activation from stimulating a single finger in spastic diplegia (Wingert et al. 2009b).

A relationship between expanded functional connectivity in spastic diplegia and clinical symptomology relies on the notion that networks of linked areas serve a collective function(s) and that significantly correlated activity indicates components with more effective synaptic interactions (Dosenbach et al. 2007; Buckner et al. 2009). Functional networks tend to verify areas with strong physiological interactions, although instances of more or less robust interactions have been noted, particularly in various disease or cognitive states (Hampson et al. 2006; Greicius et al. 2007; He et al. 2007; Buckner et al. 2008, 2009). Thus, functional networks linked to selected seed regions reliably predict cortical areas activated in task-related imaging studies even in the absence of behavioral tasks (Vincent et al. 2006, 2007); these studies include findings from somatosensory and motor cortex (Biswal et al. 1995; Cordes et al. 2000; De Luca et al. 2005; Fox et al. 2006b). Consequently, the observed functional connectivity networks in diplegia may specifically affect the processing of somatosensory inputs. Thus, activity in a somatosensory cortical area devoted to a single body region could,

through an expanded network, cascade effects across much of the body map. Furthermore, the unique processing that occurs in different S1 subdivisions might be confounded by the extensive overlap in the functional connectivity maps associated with each subdivision. Such altered somatosensory connectivity may underlay the tactile deficits observed in spastic diplegia (Wingert et al. 2008).

A possible clinical consequence suggested from the observed functional connectivity maps in diplegia is loss of coordinated messages from somatosensory to motor areas from an early age. The presence of disrupted connectivity between somatosensory and motor cortex from infancy might lead to developmental delays, abnormal sensory feedback for motor coordination (Bax et al. 2005), deficits in fine and gross motor function (Himmelmann et al. 2006), and diminished selective motor control (Ostensjo et al. 2004; Fowler et al. 2009). With damage to the subplate likely to be greater in individuals with more severe spastic diplegia symptoms (McQuillen and Ferriero 2005), more extensive functional connectivity maps are predictable. More severe symptoms are often accompanied by cognitive deficits (Bax et al. 2005). Cognitive difficulties might similarly result from expanded functional connectivity that disrupts defined linkages between cortical areas needed for effective learning and attention behavior.

Functional networks like those in the current study do not require monosynaptic anatomical connections (He et al. 2007), but may result from polysynaptic structural linkages that might involve cortical-tosubcortical connections (Vincent et al. 2007; Honey et al. 2009). In spastic diplegia, however, PWMI disrupts connections between cortex and subcortical structures (Volpe 2009), whereas many corticocortical connections persist (Hoon et al. 2002, 2009; Thomas et al. 2005; Nagae et al. 2007). Thus, the observed functional connections in diplegia are a likely consequence of strengthening normally present intracortical connections and some new intracortical, polysynaptic connections (Marin-Padilla 1997). Less probable is development of extended, direct intracortical connections because the fiber distance needed to link between different body representations within the postcentral gyrus and between pre- and postcentral gyri needed for the connectivity maps in diplegia is >5 cm, a distance that, on a theoretical basis, only weakly predicts functional connectivity data between paired regions (Honey et al. 2009). However, supporting the notion of anatomical connections is evidence that resting state functional connectivity data can predict 80% of structural connections between region pairs empirically established with tractography (Honey et al. 2009). Since functional connectivity is noninvasive and requires no or minimal tasks, it can be used to evaluate functional cortical networks involved in other abnormalities common in spastic diplegia, whether language, cognitive, or seizures, and in all severities and subtypes of cerebral palsy.

Acknowledgments

The project described was supported by Award Number R01 NS37237 from the National Institute of Neurological Disorders and Stroke. The content is solely the responsibility of the authors and does not necessarily represent the official views of the National Institute of Neurological Disorders and Stroke or the National Institutes of Health. Additional funds provided by the McDonnell Center for Higher Brain Function.

References

Back SA, Luo NL, Borenstein NS, Levine JM, Volpe JJ, Kinney HC. Late oligodendrocyte progenitors coincide with the developmental window of vulnerability for human perinatal white matter injury. J Neurosci 2001;21:1302–1312. [PubMed: 11160401]

Back SA, Luo NL, Mallinson RA, O'Malley JP, Wallen LD, Frei B, Morrow JD, Petito CK, Roberts CT Jr, Murdoch GH, et al. Selective vulnerability of preterm white matter to oxidative damage defined by F2-isoprostanes. Ann Neurol 2005;58:108–120. [PubMed: 15984031]

Bax M, Goldstein M, Rosenbaum P, Leviton A, Paneth N, Dan B, Jacobsson B, Damiano D. Proposed definition and classification of cerebral palsy, April 2005. Dev Med Child Neurol 2005;47:571–576. [PubMed: 16108461]

Ben-Ari Y. Excitatory actions of GABA during development: The nature of the nurture. Nat Rev Neurosci 2002;3:728–739. [PubMed: 12209121]

Biswal B, Yetkin FZ, Haughton VM, Hyde JS. Functional connectivity in the motor cortex of resting human brain using echo-planar MRI. Magn Reson Med 1995;34:537–541. [PubMed: 8524021]

Buckner RL, Head D, Parker J, Fotenos AF, Marcus D, Morris JC, Snyder AZ. A unified approach for morphometric and functional data analysis in young, old, and demented adults using automated atlas-based head size normalization: Reliability and validation against manual measurement of total intracranial volume. NeuroImage 2004;23:724–738. [PubMed: 15488422]

Buckner RL, Andrews-Hanna JR, Schacter DL. The brain's default network: Anatomy, function, and relevance to disease. Ann NY Acad Sci 2008;1124:1–38. [PubMed: 18400922]

Buckner RL, Sepulcre J, Talukdar T, Krienen FM, Liu H, Hedden T, Andrews-Hanna JR, Sperling RA, Johnson KA. Cortical hubs revealed by intrinsic functional connectivity: Mapping, assessment of stability, and relation to Alzheimer's disease. J Neurosci 2009;29:1860–1873. [PubMed: 19211893]

Burton H, Fabri M. Ipsilateral intracortical connections of physiologically defined cutaneous representations in areas 3b and 1 of macaque monkeys: Projections in the vicinity of the central sulcus. J Comp Neurol 1995;355:508–538. [PubMed: 7636029]

Burton H, Fabri M, Alloway K. Cortical areas within the lateral sulcus connected to cutaneous representations in areas 3b and 1: A revised interpretation of the second somatosensory area in macaque monkeys. J Comp Neurol 1995;355:539–562. [PubMed: 7636030]

Burton H, McLaren D, Sinclair R. Reading embossed capital letters: A fMRI study in blind and sighted individuals. Hum Brain Mapp 2006;27:325–339. [PubMed: 16142777]

Burton H, Wingert JR, Sinclair RJ, Dixit S. An fMRI study of cortical activity in cerebral palsy. Dev Med Child Neurol 2007;4941

Burton H, Sinclair RJ, McLaren DG. Cortical network for vibrotactile attention: A fMRI study. Hum Brain Mapp 2008a;29:207–221. [PubMed: 17390318]

Burton H, Sinclair R, Wingert J, Dierker D. Multiple parietal operculum subdivisions in humans: Tactile activation maps. Somatosens Mot Res 2008b;25:149–162. [PubMed: 18821280]

Cordes D, Haughton VM, Arfanakis K, Wendt GJ, Turski PA, Moritz CH, Quigley MA, Meyerand ME. Mapping functionally related regions of brain with functional connectivity MR imaging. AJNR Am J Neuroradiol 2000;21:1636–1644. [PubMed: 11039342]

De Luca M, Smith SM, De Stefano N, Federico A, Matthews PM. Blood oxygenation level dependent contrast resting state networks are relevant to functional activity in the neocortical sensorimotor system. Exp Brain Res 2005;167:587–594. [PubMed: 16284751]

Dosenbach NU, Fair DA, Miezin FM, Cohen AL, Wenger KK, Dosenbach RA, Fox MD, Snyder AZ, Vincent JL, Raichle ME, et al. Distinct brain networks for adaptive and stable task control in humans. Proc Natl Acad Sci USA 2007;104:11073–11078. [PubMed: 17576922]

Eickhoff SB, Grefkes C, Zilles K, Fink GR. The somatotopic organization of cytoarchitectonic areas on the human parietal operculum. Cereb Cortex 2007;17:1800–1811. [PubMed: 17032710]

Eliasson AC, Krumlinde-Sundholm L, Rosblad B, Beckung E, Arner M, Ohrvall AM, Rosenbaum P. The Manual Ability Classification System (MACS) for children with cerebral palsy: Scale development and evidence of validity and reliability. Dev Med Child Neurol 2006;48:549–554. [PubMed: 16780622]

Fowler EG, Staudt LA, Greenberg MB, Oppenheim WL. Selective Control Assessment of the Lower Extremity (SCALE): Development, validation, and interrater reliability of a clinical tool for patients with cerebral palsy. Dev Med Child Neurol 2009;51:607–614. [PubMed: 19220390]

Fox MD, Snyder AZ, Vincent JL, Corbetta M, Van Essen DC, Raichle ME. The human brain is intrinsically organized into dynamic, anticorrelated functional networks. Proc Natl Acad Sci USA 2005;102:9673–9678. [PubMed: 15976020]

Fox MD, Corbetta M, Snyder AZ, Vincent JL, Raichle ME. Spontaneous neuronal activity distinguishes human dorsal and ventral attention systems. Proc Natl Acad Sci USA 2006a;103:10046–10051. [PubMed: 16788060]

Fox MD, Snyder AZ, Zacks JM, Raichle ME. Coherent spontaneous activity accounts for trial-to-trial variability in human evoked brain responses. Nat Neurosci 2006b;9:23–25. [PubMed: 16341210]

Friston KJ, Holmes AP, Price CJ, Buchel C, Worsley KJ. Multisubject fMRI studies and conjunction analyses. NeuroImage 1999;10:385–396. [PubMed: 10493897]

Ghosh A, Shatz CJ. A role for subplate neurons in the patterning of connections from thalamus to neocortex. Development 1993;117:1031–1047. [PubMed: 8325233]

Gorter JW, Rosenbaum PL, Hanna SE, Palisano RJ, Bartlett DJ, Russell DJ, Walter SD, Raina P, Galuppi BE, Wood E. Limb distribution, motor impairment, and functional classification of cerebral palsy. Dev Med Child Neurol 2004;46:461–467. [PubMed: 15230459]

Greicius MD, Krasnow B, Reiss AL, Menon V. Functional connectivity in the resting brain: A network analysis of the default mode hypothesis. Proc Natl Acad Sci USA 2003;100:253–258. [PubMed: 12506194]

Greicius MD, Flores BH, Menon V, Glover GH, Solvason HB, Kenna H, Reiss AL, Schatzberg AF. Resting-state functional connectivity in major depression: Abnormally increased contributions from subgenual cingulate cortex and thalamus. Biol Psychiatry 2007;62:429–437. [PubMed: 17210143]

Hampson M, Peterson BS, Skudlarski P, Gatenby JC, Gore JC. Detection of functional connectivity using temporal correlations in MR images. Hum Brain Mapp 2002;15:247–262. [PubMed: 11835612]

Hampson M, Driesen NR, Skudlarski P, Gore JC, Constable RT. Brain connectivity related to working memory performance. J Neurosci 2006;26:13338–13343. [PubMed: 17182784]

He BJ, Snyder AZ, Vincent JL, Epstein A, Shulman GL, Corbetta M. Breakdown of functional connectivity in frontoparietal networks underlies behavioral deficits in spatial neglect. Neuron 2007;53:905–918. [PubMed: 17359924]

Himmelmann K, Hagberg G, Beckung E, Hagberg B, Uvebrant P. The changing panorama of cerebral palsy in Sweden. IX. Prevalence and origin in the birth-year period 1995–1998. Acta Paediatr 2005;94:287–294. [PubMed: 16028646]

Himmelmann K, Beckung E, Hagberg G, Uvebrant P. Gross and fine motor function and accompanying impairments in cerebral palsy. Dev Med Child Neurol 2006;48:417–423. [PubMed: 16700930]

Holmes AP, Friston KJ. Generalisability, random effects and population inference. NeuroImage 1998;7:S754.

Honey CJ, Sporns O, Cammoun L, Gigandet X, Thiran JP, Meuli R, Hagmann P. Predicting human resting-state functional connectivity from structural connectivity. Proc Natl Acad Sci USA 2009;106:2035–2040. [PubMed: 19188601]

Hoon AH Jr, Lawrie WT Jr, Melhem ER, Reinhardt EM, van Zijl PCM, Solaiyappan M, Jiang H, Johnston MV, Mori S. Diffusion tensor imaging of periventricular leukomalacia shows affected sensory cortex white matter pathways. Neurology 2002;59:752–756. [PubMed: 12221171]

Hoon AH Jr, Stashinko EE, Nagae LM, Lin DD, Keller J, Bastian A, Campbell ML, Levey E, Mori S, Johnston MV. Sensory and motor deficits in children with cerebral palsy born preterm correlate with diffusion tensor imaging abnormalities in thalamocortical pathways. Dev Med Child Neurol 2009;51:697–704. [PubMed: 19416315]

Huang ZJ, Di Cristo G, Ango F. Development of GABA innervation in the cerebral and cerebellar cortices. Nat Rev Neurosci 2007;8:673–686. [PubMed: 17704810]

Jenkins, GM.; Watts, DG. Spectral analysis and its applications. Boca Raton: Emerson-Adams Press; 1968.

Jones EG, Powell TPS. Connexions of the somatic sensory cortex of the rhesus monkey. I. Ipsilateral cortical connexions. Brain 1969;92:477–502. [PubMed: 4979846]

Jones EG, Powell TPS. An anatomical study of converging sensory pathways within the cerebral cortex of the monkey. Brain 1970;93:793–820. [PubMed: 4992433]

Kanold PO, Kara P, Reid RC, Shatz CJ. Role of subplate neurons in functional maturation of visual cortical columns. Science 2003;301:521–525. [PubMed: 12881571]

Kanold PO, Shatz CJ. Subplate neurons regulate maturation of cortical inhibition and outcome of ocular dominance plasticity. Neuron 2006;51:627–638. [PubMed: 16950160]

Korzeniewski SJ, Birbeck G, DeLano MC, Potchen MJ, Paneth N. A systematic review of neuroimaging for cerebral palsy. J Child Neurol 2008;23:216–227. [PubMed: 18263759]

Kostovic I, Jovanov-Milosevic N. Subplate zone of the human brain: Historical perspective and new concepts. Coll Antropol 2008;32:3–8. [PubMed: 18405051]

Kuban KC, Leviton A. Cerebral palsy. N Engl J Med 1994;330:188–195. [PubMed: 8264743]

Kulak W, Sobaniec W, Kubas B, Walecki J, Smigielska-Kuzia J, Bockowski L, Artemowicz B, Sendrowski K. Spastic cerebral palsy: Clinical magnetic resonance imaging correlation of 129 children. J Child Neurol 2007;22:8–14. [PubMed: 17608298]

Kwong KK, Belliveau JW, Chesler DA, Goldberg IE, Weisskoff RM, Poncelet BP, Kennedy DN, Hoppel BE, Cohen MS, Turner R, et al. Dynamic magnetic resonance imaging of human brain activity during primary sensory stimulation. Proc Natl Acad Sci USA 1992;89:5675–5679. [PubMed: 1608978]

Lancaster JL, Glass TG, Lankipalli BR, Downs H, Mayberg H, Fox PT. A modality-independent approach to spatial normalization of tomographic images of the human brain. Hum Brain Mapp 1995;3:209–223.

Leviton A, Gressens P. Neuronal damage accompanies perinatal white-matter damage. Trends Neurosci 2007;30:473–478. [PubMed: 17765331]

Maldjian JA, Gottschalk A, Patel RS, Detre JA, Alsop DC. The sensory somatotopic map of the human hand demonstrated at 4 Tesla. NeuroImage 1999;10:55–62. [PubMed: 10385581]

Marin-Padilla M. Developmental neuropathology and impact of perinatal brain damage. II: White matter lesions of the neocortex. J Neuropathol Exp Neurol 1997;56:219–235. [PubMed: 9056536]

McQuillen PS, Sheldon RA, Shatz CJ, Ferriero DM. Selective vulnerability of subplate neurons after early neonatal hypoxia-ischemia. J Neurosci 2003;23:3308–3315. [PubMed: 12716938]

McQuillen PS, Ferriero DM. Perinatal subplate neuron injury: Implications for cortical development and plasticity. Brain Pathol 2005;15:250–260. [PubMed: 16196392]

Nagae LM, Hoon AH Jr, Stashinko E, Lin D, Zhang W, Levey E, Wakana S, Jiang H, Leite CC, Lucato LT, et al. Diffusion tensor imaging in children with periventricular leukomalacia: Variability of injuries to white matter tracts. AJNR Am J Neuroradiol 2007;28:1213–1222. [PubMed: 17698519]

Nichols TE, Holmes AP. Nonparametric permutation tests for functional neuroimaging: A primer with examples. Hum Brain Mapp 2002;15:1–25. [PubMed: 11747097]

Nordahl CW, Dierker D, Mostafavi I, Schumann CM, Rivera SM, Amaral DG, Van Essen DC. Cortical folding abnormalities in autism revealed by surface-based morphometry. J Neurosci 2007;27:11725–11735. [PubMed: 17959814]

Ogawa S, Tank DW, Menon R, Ellerman JM, Kim SG, Merkle HH, Ugurbil K. Intrinsic signal changes accompanying sensory stimulation: Functional brain mapping with magnetic resonance imaging. Proc Natl Acad Sci USA 1992;89:5951–5955. [PubMed: 1631079]

Ohshiro T, Weliky M. Subplate neurons foster inhibition. Neuron 2006;51:524–526. [PubMed: 16950151]

Ojemann JG, Akbudak E, Snyder AZ, McKinstry RC, Raichle ME, Conturo TE. Anatomic localization and quantitative analysis of gradient refocused echo-planar fMRI susceptibility artifacts. NeuroImage 1997;6:156–167. [PubMed: 9344820]

Ostensjo S, Carlberg EB, Vollestad NK. Motor impairments in young children with cerebral palsy: Relationship to gross motor function and everyday activities. Dev Med Child Neurol 2004;46:580–589. [PubMed: 15344517]

Palisano RJ, Hanna SE, Rosenbaum PL, Russell DJ, Walter SD, Wood EP, Raina PS, Galuppi BE. Validation of a model of gross motor function for children with cerebral palsy. Phys Ther 2000;80:974–985. [PubMed: 11002433]

Pearson RCA, Powell TPS. The projection of the primary somatic sensory cortex upon area 5 in the monkey. Brain Res Rev 1985;9:89–107.

Quigley M, Cordes D, Wendt G, Turski P, Moritz C, Haughton V, Meyerand ME. Effect of focal and nonfocal cerebral lesions on functional connectivity studied with MR imaging. AJNR Am J Neuroradiol 2001;22:294–300. [PubMed: 11156772]

Randolph M, Semmes J. Behavioral consequences of selective subtotal ablations in the postcentral gyrus of *Macaca mulatta*. Brain Res 1974;70:55–70. [PubMed: 4207050]

Robinson S, Li Q, Dechant A, Cohen ML. Neonatal loss of gamma-aminobutyric acid pathway expression after human perinatal brain injury. J Neurosurg 2006;104:396–408. [PubMed: 16776375]

Rosenbaum PL, Walter SD, Hanna SE, Palisano RJ, Russell DJ, Raina P, Wood E, Bartlett DJ, Galuppi BE. Prognosis for gross motor function in cerebral palsy: Creation of motor development curves. JAMA 2002;288:1357–1363. [PubMed: 12234229]

Sanger TD, Kukke SN. Abnormalities of tactile sensory function in children with dystonic and diplegic cerebral palsy. J Child Neurol 2007;22:289–293. [PubMed: 17621498]

Shanks MF, Pearson RCA, Powell TPS. The ipsilateral cortico-cortical connexions between the cytoarchitectonic subdivisions of the primary somatic sensory cortex in monkey. Brain Res Rev 1985;9:67–88.

Sigurdardóttir S, Thórkelsson T, Halldórsdóttir M, Thorarensen O, Vik T. Trends in prevalence and characteristics of cerebral palsy among Icelandic children born 1990 to 2003. Dev Med Child Neurol 2009;51:356–363. [PubMed: 19388148]

Talairach, J.; Tournoux, P. Coplanar stereotaxic atlas of the human brain. New York: Thieme Medical; 1988.

Thomas B, Eyssen M, Peeters R, Molenaers G, Van Hecke P, De Cock P, Sunaert S. Quantitative diffusion tensor imaging in cerebral palsy due to periventricular white matter injury. Brain 2005;128:2562–2577. [PubMed: 16049045]

Van Essen DC, Drury HA, Dickson J, Harwell J, Hanlon D, Anderson CH. An integrated software suite for surface-based analyses of cerebral cortex. J Am Med Inform Assoc 2001;8:443–459. [PubMed: 11522765]

Van Essen DC. A population-average, landmark- and surface-based (PALS) atlas of human cerebral cortex. NeuroImage 2005;28:635–662. [PubMed: 16172003]

Van Essen DC, Dierker DL. Surface-based and probabilistic atlases of primate cerebral cortex. Neuron 2007;56:209–225. [PubMed: 17964241]

Vincent JL, Snyder AZ, Fox MD, Shannon BJ, Andrews JR, Raichle ME, Buckner RL. Coherent spontaneous activity identifies a hippocampal-parietal memory network. J Neurophysiol 2006;96:3517–3531. [PubMed: 16899645]

Vincent JL, Patel GH, Fox MD, Snyder AZ, Baker JT, Van Essen DC, Zempel JM, Snyder LH, Corbetta M, Raichle ME. Intrinsic functional architecture in the anaesthetized monkey brain. Nature 2007;447:83–86. [PubMed: 17476267]

Vincent JL, Kahn I, Snyder AZ, Raichle ME, Buckner RL. Evidence for a frontoparietal control system revealed by intrinsic functional connectivity. J Neurophysiol 2008;100:3328–3342. [PubMed: 18799601]

Volpe JJ. Brain injury in premature infants: A complex amalgam of destructive and developmental disturbances. Lancet Neurol 2009;8:110–124. [PubMed: 19081519]

Vry J, Linder-Lucht M, Berweck S, Bonati U, Hodapp M, Uhl M, Faist M, Mall V. Altered cortical inhibitory function in children with spastic diplegia: A TMS study. Exp Brain Res 2008;186:611–618. [PubMed: 18214452]

Wingert JR, Burton H, Sinclair RJ, Brunstrom JE, Damiano DL. Tactile sensory abilities in cerebral palsy: Deficits in roughness and object discriminations. Dev Med Child Neurol 2008;50:1–7. [PubMed: 18754926]

Wingert JR, Burton H, Sinclair RJ, Brunstrom JE, Damiano DL. Joint-position sense and kinesthesia in cerebral palsy. Arch Phys Med Rehabil 2009a;90:447–453. [PubMed: 19254610]

Wingert JR, Sinclair RJ, Dixit S, Damiano DL, Burton H. Somatosensory-evoked cortical activity in spastic diplegic cerebral palsy: A functional MR imaging study. Hum Brain Mapp. 2009b (under review).

Zecevic N, Chen Y, Filipovic R. Contributions of cortical subventricular zone to the development of the human cerebral cortex. J Comp Neurol 2005;491:109–122. [PubMed: 16127688]

Appendix: Abbreviations

API	Area-proportion index
ACR	Auto-correlation function
BOLD	Blood oxygenation level dependent

BA	Brodmann area
CP	Cerebral palsy
CMs	Conjunction maps
FCN	Controls
FCCP	Diplegia
TE	Echo time
EPI	Echo-planar sequences
fcMRI	Functional connectivity analyses
fMRI	Functional magnetic resonance imaging
GF	Gamma factor
IPS	Intraparietal sulcal cortex
LTD	Long-term depression
MP-RAGE	Magnetization prepared rapid gradient echo
PO	Parietal operculum
OP 1	Parietal operculum subdivision 1
PWMI	Periventricular white-matter injury
PCG	Postcentral gyrus
S1	Primary somatosensory cortex
ROI	Region of interest
TR	Repetition time
S2	Second somatosensory cortex
sROI	Seed ROI
STDP	Spike timing-dependent plasticity

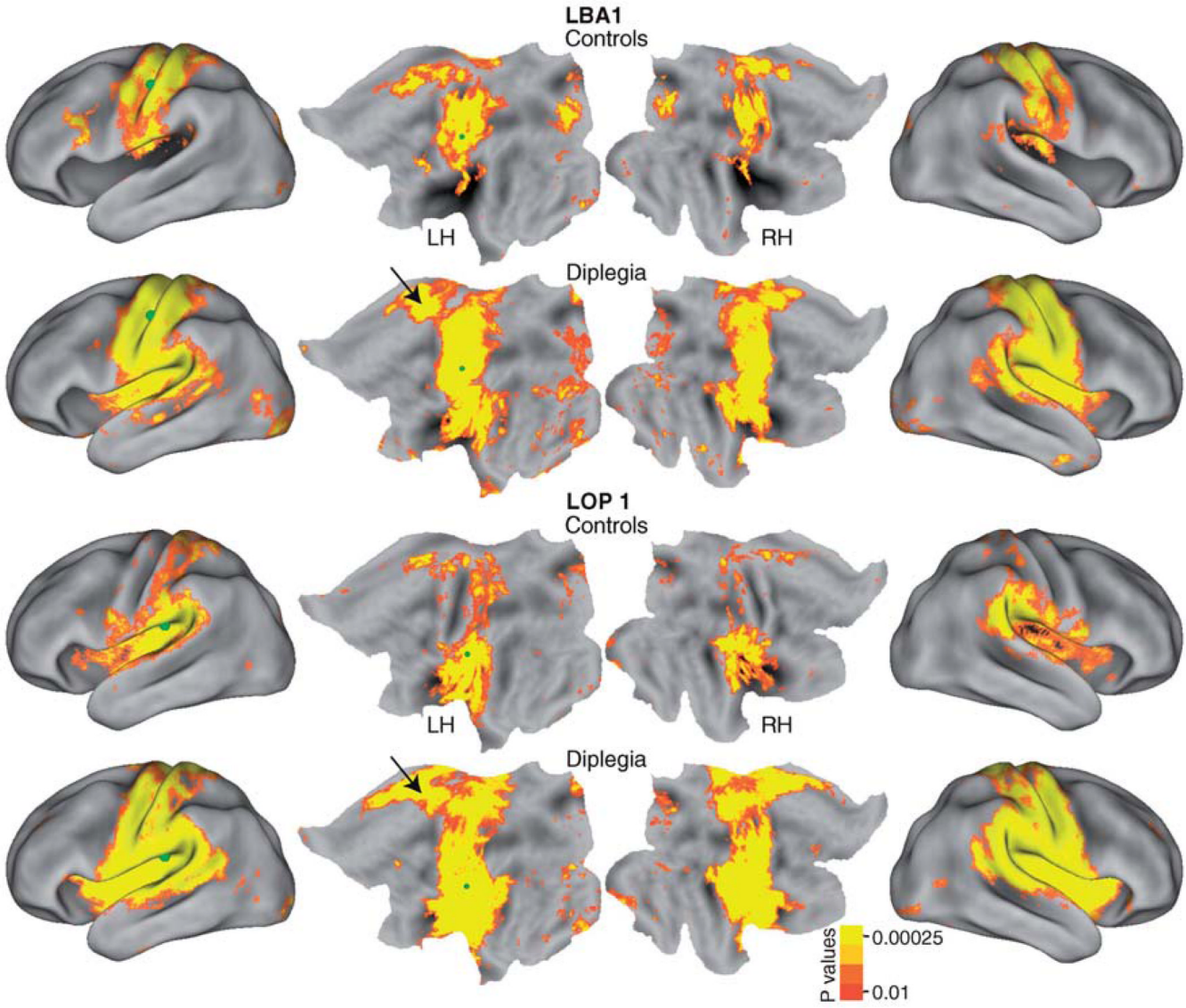

Figure 1.

Functional connectivity maps for left hemisphere somatosensory seed regions (L BA1 and L OP 1). Random effect *t*-maps of *r*- to *Z*-transformed averages per group. Seed locations are marked with green spheres.

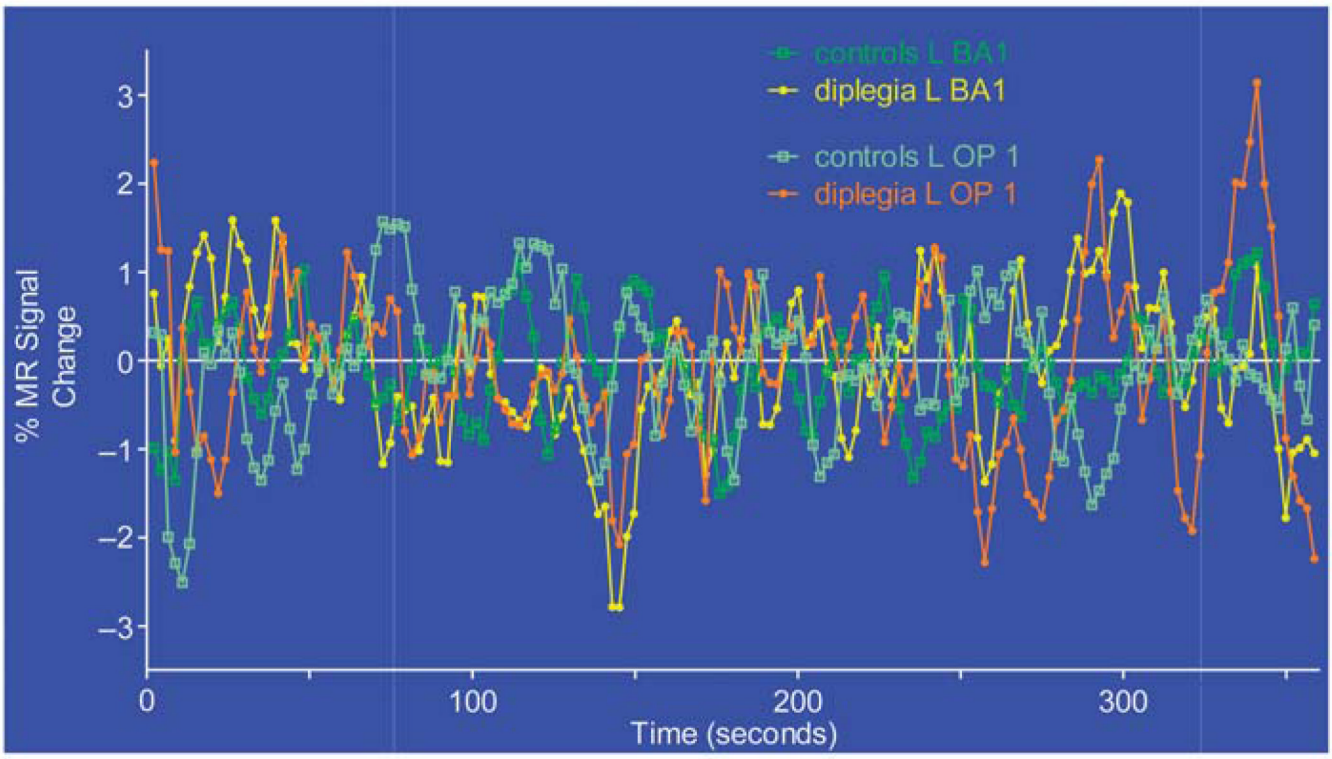

Figure 2.
Average resting state MR signal timecourse from seed regions L BA1 and L OP 1 in diplegia and control groups.

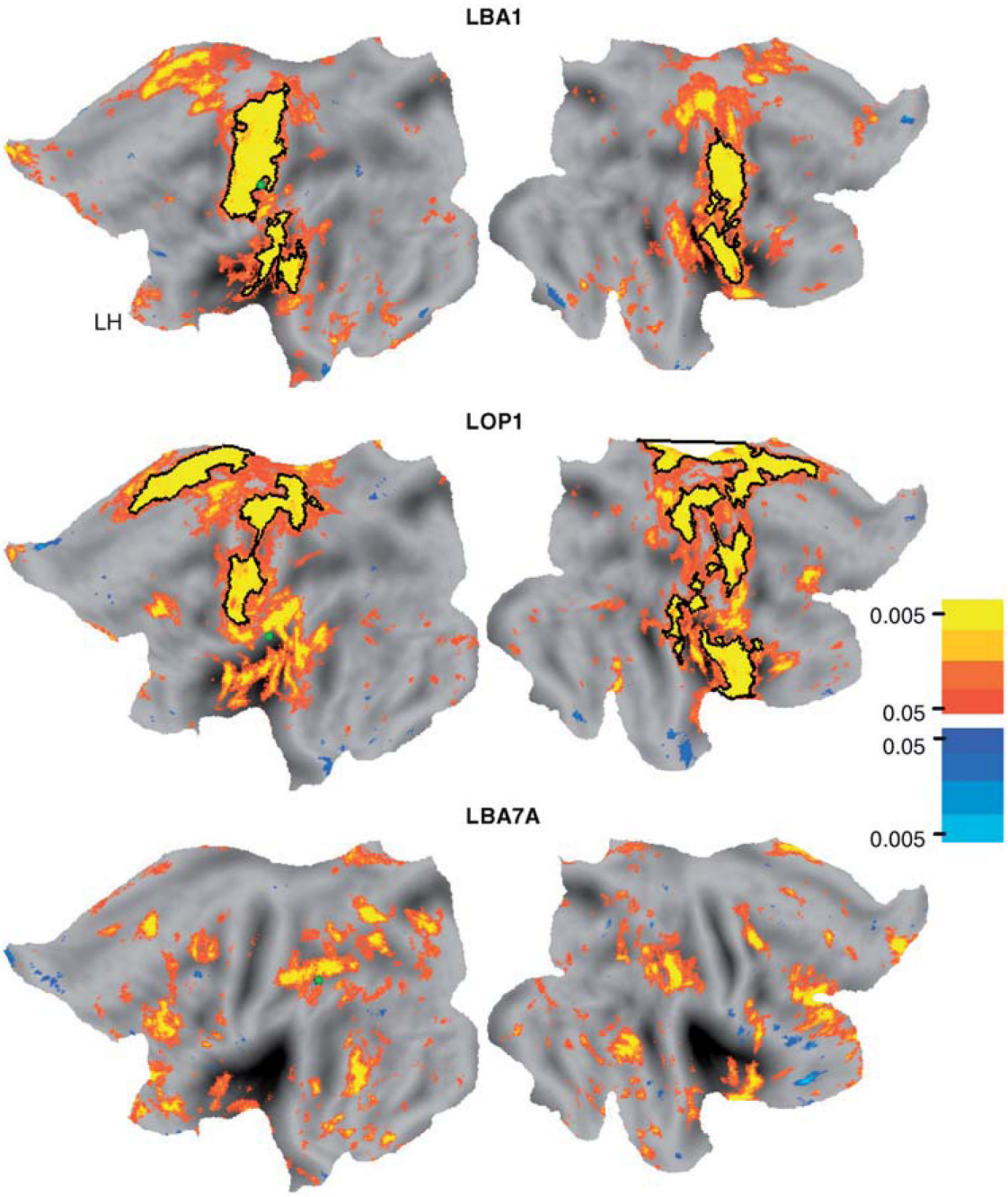

Figure 3.
Group contrasts (*t*-test maps) of functional connectivity results for different seed regions (L BA1, L OP 1, and L BA7A). Black borders surround regions where permutation analyses (Nordahl et al. 2007) indicated significant group differences in functional connectivity maps (see Methods).

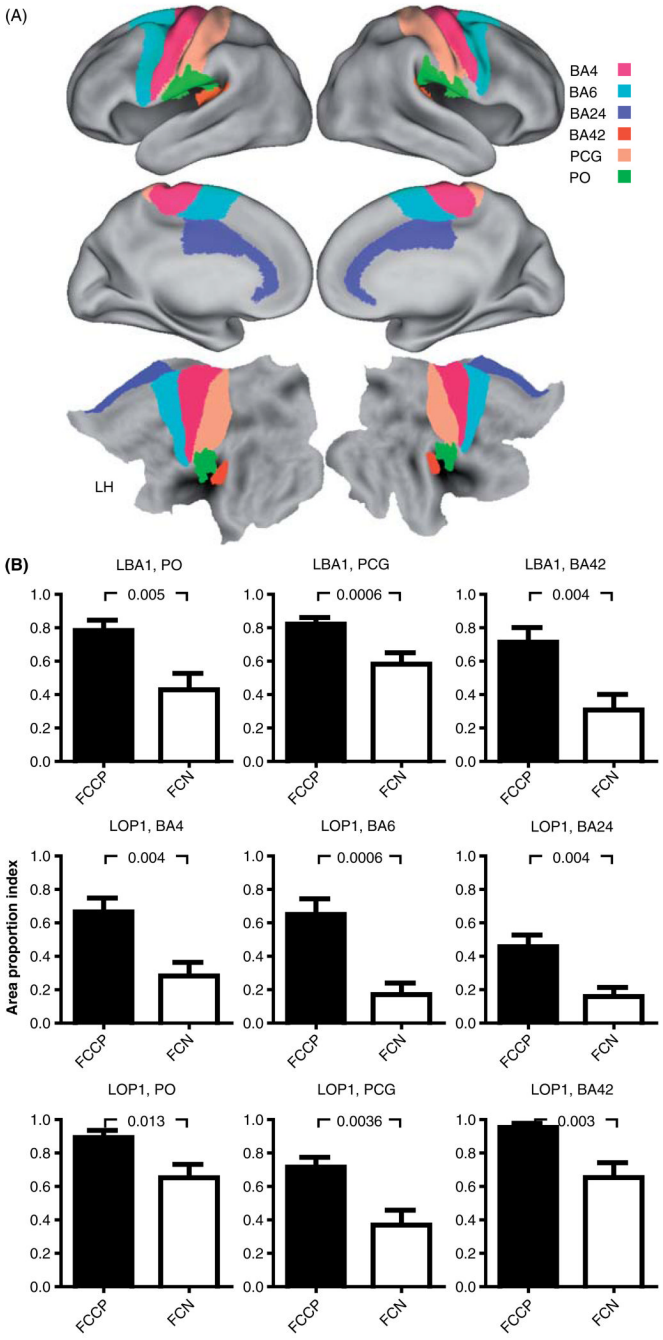

Figure 4.

Average area-proportion indices per group. (A) Selected cortical areas used for area extent analyses. Top two rows show average inflated cortical surface and bottom row shows flattened surface from PALS-B12 atlas (Van Essen 2005; Van Essen and Dierker 2007). Boundary of postcentral gyrus (PCG) based on conjunction of Brodmann areas 3, 1, and 2. These and other BA borders were based on maps from the PALS-B12 atlas. Boundary of parietal operculum (PO) based on conjunction of OP subdivisions 1, 3, and 4 (Burton et al. 2008b). (B) Area proportions for seed regions in left primary and secondary somatosensory cortex, L BA1 and L OP 1, respectively. *p*-Values of group contrast *t*-test results are noted above graphs. All group contrast *t*-test results were significant. Error bars are SEMs. Abbreviations: BA4, Brodmann

area 4; BA6, Brodmann area 6; BA24, Brodmann area 24; BA42, Brodmann area 42 (primary auditory); PCG, postcentral gyrus; PO, parietal operculum; FCCP, diplegia; FCN, controls.

Table I

Coordinates of parietal cortex seed regions of interest.

Seed regions		*x*	*y*	*z*
Left postcentral sulcus	L BA3	−47	−19	36
Right postcentral sulcus	R BA3	40	−18	40
Left postcentral gyrus	L BA1	−50	−21.4	45
Right postcentral gyrus	R BA1	50	−15.4	45.5
Left posterior postcentral gyrus	L BA2	−48	−31.7	42
Right posterior postcentral gyrus	R BA2	43.5	−27.5	45.4
Left parietal operculum	L OP 1	−50	−27.5	19
Left medial postcentral gyrus	L BA5	−28.8	−50.7	60
Left inferior intraparietal sulcus	L BA7A	−42.5	−48.4	42.1
Right inferior intraparietal sulcus	R BA7A	40.1	−45	45
Left superior intraparietal sulcus	L BA7P	−28.4	−61.4	46.3
Right superior intraparietal sulcus	R BA7P	27.4	−58	48

Table II

Location and size of clusters where functional connectivity maps by seed ROI were significantly larger in diplegia vs controls.

Seed: Seed ROI	Cluster location	Cluster size threshold (mm^2)	Cluster size in mm^2 (*p*-value)	Stereotaxic coordinates		
				X	*Y*	*Z*
L BA3	LH-pre-postcentral gyri	698.9	3346.0 (0.006)	−39.1	−23.5	42.8
	RH-pre-postcentral gyri + parietal operculum	797	4811.6 (0.006)	38	−18.8	40.4
R BA3	LH-pre-postcentral gyri	781.1	1555.6 (0.02)	−35.6	−25.3	55.4
	RH-pre-postcentral gyri + parietal operculum + insula	801.2	8057.9 (0.005)	35.5	−18.5	41.1
L BA1	LH-pre-postcentral gyri	827	3376.1 (0.01)	−37.2	−24.1	52.1
	LH-parietal operculum + Heschl's gyrus	827	1769.8 (0.02)	−46.2	−28.8	13.4
	RH-pre-postcentral gyri, parietal operculum + insula	775.8	3440.5 (0.01)	44.7	−12	30.6
R BA1	LH	802.8	NS			
	RH-pre-postcentral gyri + parietal operculum + insula	897.1	4481.7 (0.007)	42.4	−8.7	23
L BA2	LH	713.3	NS			
	RH-medial postcentral + superior parietal lobule	700.7	1280.6 (0.02)	25.3	−42.4	58.8
R BA2	LH	879.7	NS			
	RH-superior parietal lobule	853	1094.9 (0.04)	25	−41.4	60.8
L BA5	LH	744	NS			
	RH-medial postcentral + superior parietal lobule	772.7	1583.3 (0.02)	26.6	−45	56.1
	RH-superior parietal lobule	772.7	793.6 (0.05)	19.2	−70.6	42.8
L OP 1	LH-pre-postcentral gyri	951.3	2592.1 (0.01)	−31.8	−28.5	52.9
	LH-medial frontal cortex	951.3	1347.2 (0.03)	−10.9	−19.1	42.9
	RH-medial frontal + postcentral gyrus	927.3	2075.1 (0.02)	6.9	−21.7	50.9
	RH-pre-postcentral gyri + premotor	927.3	1487.6 (0.03)	37.5	−14.7	48.8
	RH-insula	927.3	1376.3 (0.03)	35.6	0.4	6.2
	RH-parietal operculum + SMG + HG	927.3	1322.6 (0.03)	55.2	−29.6	25.5
	RH-medial paracentral + superior parietal lobule	927.3	1160 (0.04)	17.4	−37.6	64.7
L BA7A	LH	612.4	NS			
	RH	706.7	NS			

Seed: Seed ROI	Cluster location	Cluster size threshold (mm^2)	Cluster size in mm^2 (p-value)	Stereotaxic coordinates		
				X	*Y*	*Z*
R BA7A	LH-intraparietal sulcal cortex	657.4	695.1 (0.047)	−34.2	−53.1	47.4
	RH-intraparietal sulcal cortex	618.2	958 (0.025)	43.5	−33.8	44.5
L BA7P	LH-precuneus	707.2	807 (0.04)	−8.8	−74	38
	LH-dorsolateral prefrontal cortex	707.2	748 (0.050)	−39.4	35.7	19.7
	RH-superior temporal gyrus + sulcus	678.8	795 (0.04)	58.7	−41.5	−8.2
R BA7P	LH	740.6	NS			
	RH-intraparietal sulcal cortex	713.1	770.6 (0.044)	35	−44.1	46.3
	RH-superior parietal lobule	713.1	741.4 (0.048)	17.3	−69.3	48.5

Table III

p-Values for *post hoc t*-tests of group differences in area-proportion indices.

Seed	PO[a]	PCG	BA6	BA42	BA4	BA24
Selected region in left hemisphere						
L BA3	0.005*	0.009	0.090	0.001*	0.009	0.036
L BA1	0.005*	0.005*	0.321	0.004*	0.012	0.011
L BA2	0.170	0.026	0.101	0.236	0.032	0.014
L OP 1	0.013	0.004*	0.001*	0.003*	0.004*	0.004*
L BA7A	0.853	0.894	0.666	0.964	0.862	0.785
Selected region in right hemisphere						
L BA3	0.005*	0.009	0.094	0.001*	0.009	0.054
L BA1	0.003*	0.006*	0.107	0.007*	0.011	0.017
L BA2	0.123	0.040	0.106	0.297	0.036	0.033
L OP 1	0.027	0.004*	0.068	0.005*	0.005*	0.008*
L BA7A	0.744	0.816	0.715	0.989	0.836	0.816

[a]Selected regions: PO = second somatosensory/parietal operculum; PCG = primary somatosensory/postcentral gyrus; BA42 = primary auditory; BA4 = primary motor; BA6 = premotor; BA24 = cingulate cortex.

*p-Values in shaded cells were significant after Bonferroni correction for six selected regions (0.05/6 = 0.008).